694 J. Opt. Soc. Am. A/Vol. 3, No. 5/May 1986

Effect of aberrations and apodization on the performance of coherent optical systems. I. The amplitude impulse response

J. P. Mills* and B. J. Thompson

Institute of Optics, University of Rochester, Rochester, New York 14627

Received July 18, 1985; accepted December 5, 1985

A systematic study was performed in which the effects of aberrations and apodization on the performance of a coherent optical system were investigated. The system performance was characterized by the modulus and the phase of the amplitude impulse response. The aberrations considered were defocus, spherical aberration, coma, and astigmatism. The apodizer was Gaussian in amplitude transmittance. The results of the study indicate that, within certain limits, the apodizer was effective in removing the sidelobes from the aberrated amplitude impulse response. This has significant implications for the performance of coherent imaging and beam-propagation systems.

INTRODUCTION

The importance of coherent optical systems has grown dramatically since the inception of the laser. At present a great variety of coherent optical systems exist in research, industrial, government, and business applications. For the purpose of this paper, these coherent systems can be divided into two broad categories: (1) image-forming systems and (2) beam-propagation and -focusing systems. Examples of image-forming systems include optical data storage and retrieval, optical image processing, and some microscopy. Laser welding, eye surgery, and high-power lasers for fusion research are examples of beam-focusing systems.

A common feature of all these systems is the presence of optical aberrations. Even in the most highly corrected systems, such as those used in photomicrolithography, there are some residual aberrations; and most systems are not so well corrected. Those systems that were relatively well corrected in the design phase can have additional aberrations introduced by the manufacturing process and environmental stresses. Aberrations result in phase errors in the imaging (or beam-propagation) wave front as it traverses the optical system. These errors have well-known effects on the performance of these systems.[1–4] The usual response from an optical designer when an aberration has resulted in an unacceptable degradation of performance is to alter the surface contours of the optical elements in the optical system to decrease the overall amount of aberrations. It will be shown that the use of apodization is also useful in controlling the effects of aberrations in coherent systems.

Apodization is the deliberate modification of the transmittance of the optical system. This modification results in a significantly altered system impulse response, which in turn affects the imaging or beam-propagation characteristics of the optical system. For aberrated incoherent optical systems, the use of apodization has theoretically been shown to moderate the deleterious effects of the aberrations on system performance.[2–11] However, the use of apodization to improve the performance of aberrated coherent optical systems has apparently not been studied.

The work reported here seeks to fill that void. A systematic study was performed investigating the effects of aberrations and apodization (separately and in combination) on selected aspects of the performance of coherent optical systems. The present paper reports the results of the portion of the study related to the amplitude impulse response, which is the fundamental function of importance in coherent and partially coherent systems. (For incoherent systems it is the irradiance impulse response that is the fundamental function; the irradiance impulse response is the product of the amplitude impulse response with its complex conjugate.) Future papers will address the analogous aspects of coherent imaging systems and coherent beam-propagation systems.

THEORY

The amplitude impulse response is defined as the complex optical field amplitude in the image plane of an optical system when the object is a point source of unit amplitude and zero phase. In the presence of aberrations other than defocus, the image plane is the one in which the best Strehl ratio is obtained. In the case of defocus, the image plane is the one determined by geometrical optics.

Theoretical Development

The effects of aberrations and apodization were investigated theoretically by considering the idealized optical system shown in Fig. 1. In the object plane, an on-axis point source radiates a diverging spherical wave. The lens L1, a distance from the object plane equal to its focal length f_1, collimates the diverging spherical wave. The lens L1 is assumed to produce a perfectly collimated wave front. This assumption is the usual one in which all the diffraction effects are associated with the limiting aperture of the system. The (x_1, y_1) plane is a distance $f_1 + f_2$ away from lens L1 and a distance f_2 away from image plane, where f_2 is the focal length of lens L2. The apodizer, the lens L2, and the limiting aperture were all assumed to be coincident with the (x_1, y_1) plane, which is also the exit pupil of the system. The transmittance of the exit pupil can then be described by

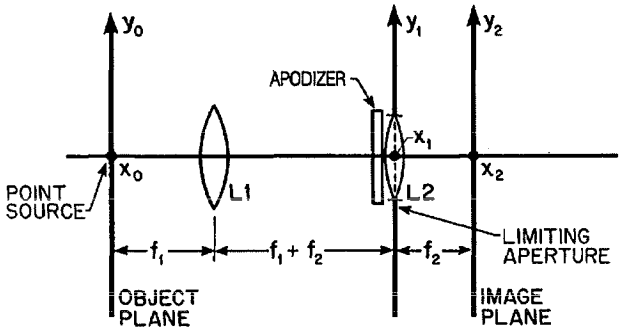

Fig. 1. The geometry of the analyzed coherent optical system.

$$T(x_1, y_1) = A(x_1, y_1)\exp\left[\frac{-i\pi}{\lambda f_2}(x_1^2 + y_1^2)\right] \times \exp\left[\frac{-i2\pi}{\lambda f_2}\Phi(x_1, y_1)\right]B(x_1, y_1), \quad (1)$$

where $A(x_1, y_1)$ is the amplitude transmittance of the apodizer, f_2 is the focal length of lens L2, and λ is the illumination wavelength. The first exponential term accounts for the modification of the wave front by a perfect thin lens, the second exponential term accounts for the aberration introduced by a real lens, and $B(x_1, y_1)$ represents the finite extent of the limiting aperture.

The apodization used in this study had an amplitude transmittance that was Gaussian in form:

$$A(x_1, y_1) = \exp[-3(x_1^2 + y_1^2)] = \exp(-3r^2), \quad (2)$$

where the constant in the exponent was chosen so that the value of $A(x_1, y_1)$ at the edge of the limiting aperture was equal to 0.050. This function is displayed in Fig. 2 as a solid curve. The dashed curve in this figure represents the amplitude transmittance of the unapodized limiting aperture.

The reason for selecting a Gaussian apodization was that it was desirable to have an apodizer that produced a real and positive amplitude impulse response.[12] Many of the deleterious effects seen in coherent imaging (edge ringing, for example) occur because the amplitude impulse response has negative regions. By contrast, an incoherent system has an impulse response that is always real and positive. This observation led to the conclusion that it would be appropriate to make the amplitude impulse response for the coherent case real and positive as well. The amplitude impulse response of an optical system is proportional to the Fourier transform of the optical field in the exit pupil of the system. So, if the transmittance of the apodizer has the functional form of a Gaussian truncated far from its center, then the amplitude impulse response will be nearly real and positive.

The aberrations considered were those described by the Siedel wave front representation[13]

$$\Phi(r, \theta) = a_{20}r^2 + a_{40}r^4 + a_{31}r^3\cos\theta + a_{22}r^2\cos^2\theta, \quad (3)$$

where a_{20}, a_{40}, a_{31}, and a_{22} are the amounts of defocus, spherical aberration, coma, and astigmatism, respectively. The quantities r and θ are defined by

$$r^2 = x_1^2 + y_1^2, \qquad \theta = \tan^{-1}(y_1/x_1).$$

The image-plane optical field arising from the point source is proportional to the two-dimensional Fourier transform of the exit pupil field distribution[14]

$$K(x_2, y_2) = \frac{1}{\lambda^2 f_2^2}\int\int_{-\infty}^{\infty} T(x_1, y_1) \times \exp\left[\frac{-i2\pi}{\lambda f_2}(x_1x_2 + y_1y_2)\right]dx_1dy_1. \quad (4)$$

$K(x_2, y_2)$ then is the expression for the amplitude impulse response of the idealized optical system of Fig. 1.

There are several assumptions implicit in Eq. (4). It was assumed that a scalar diffraction treatment of this problem was sufficient. Also, the usual paraxial assumptions were made, namely, the diameter of the exit pupil was much greater than the wavelength of illumination and the maximum linear distance in the region of interest in the image plane was much less than the distance from the exit pupil to the image plane.

Noting that these assumptions are valid in most optical systems, Eq. (4) was used to calculate the amplitude impulse response for the system in the presence of various amounts of defocus and the third-order aberrations, both with and without the Gaussian apodization.

Theoretical Data

Equation (4) was computed on a VAX 11/750 computer using a fast-Fourier-transform subroutine from the IMSL[14] package.

The quantity $K(x_2, y_2)$ in Eq. (4) is, in general, complex. Consequently, the output of the program is in terms of real and imaginary coefficients, i.e.,

$$K(x_2, y_2) = a(x_2, y_2) + ib(x_2, y_2) = m(x_2, y_2)\exp[ip(x_2, y_2)], \quad (5)$$

where $a(x_2, y_2)$ and $b(x_2, y_2)$ are the coefficients and $m(x_2, y_2)$

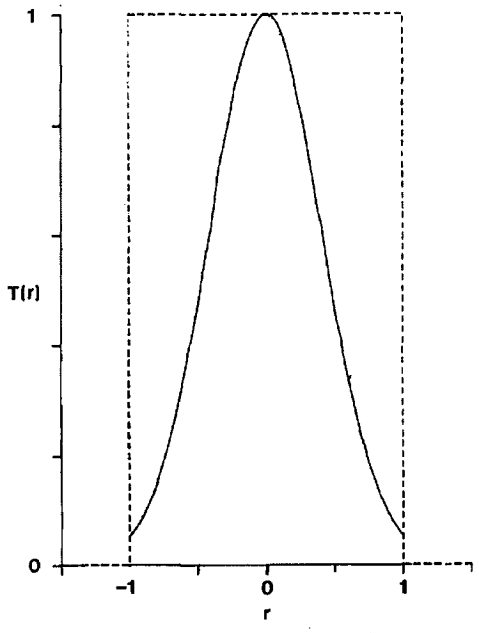

Fig. 2. The amplitude transmittance $T(r)$ of the Gaussian filter used in this study (solid curve) shown relative to the unapodized amplitude transmittance of the exit pupil (dashed curve).

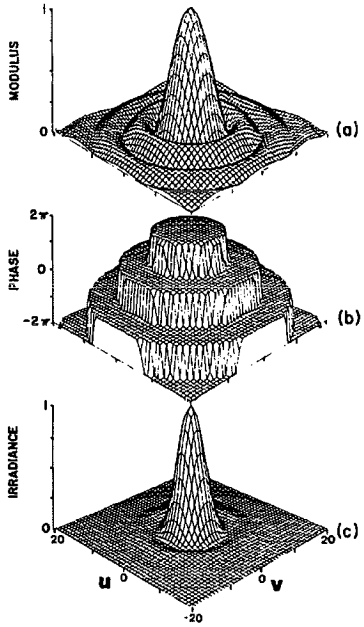

Fig. 3. The impulse response of an unaberrated, unapodized, circularly symmetric optical system in terms of (a) modulus, (b) phase, and (c) irradiance. The u and v axes are in terms of canonical distance coordinates. All plots have the same distance scales.

and $p(x_2, y_2)$ are the modulus and the phase, respectively, of the amplitude impulse response.

Coherently illuminated systems are linear in complex amplitude. However, if measurements are to be made in an experiment, it is the irradiance $I(x_2, y_2)$ that is usually measured. The irradiance of the amplitude impulse response is related to its complex amplitude by

$$I(x_2, y_2) = K(x_2, y_2)K^*(x_2, y_2) = |K(x_2, y_2)|^2, \qquad (6)$$

where the asterisk denotes the complex conjugate.

A typical output of this program is displayed in Fig. 3. The system in this case was unaberrated and unapodized, and the pupil function was a circular aperture. The distance coordinates used in Fig. 3, as well as in many other figures in this paper, are the canonical distance coordinates u and v, defined by

$$u = \frac{2\pi a}{d_i} x_i, \qquad v = \frac{2\pi a}{d_i} y_i, \qquad (7)$$

where a is the radius of the exit pupil, d_i is the distance from the exit pupil to the image plane, and x_i and y_i are the spatial coordinates in the image plane.

A coherent optical system is linear in field amplitude, which is a complex quantity. So, unlike in an incoherent system, the phase in the optical field is critically important in determining the final image irradiance distribution. For this reason, the phase was calculated for the unaberrated case and is displayed in Fig. 3(b). The phase was also calculated for many of the aberrated cases considered later.

The phase distribution in the amplitude impulse response of an unaberrated system [see Fig. 3(b)] is uniform everywhere except along concentric circles, where the phase jumps discontinuously by an amount equal to π rad. These jumps occur at the same spatial locations as do the zero values in the modulus distribution of Fig. 3(a). This implies that in every other ring the amplitude impulse response is composed of negative values. It is these negative regions that cause the ringing phenomenon seen in the image of an edge.

The irradiance distribution of this impulse response is shown in Fig. 3(c). It is obtained by squaring the modulus distribution. Since the optical system in this case is unaberrated and has a circular exit pupil, it is expected that the irradiance distribution would approximate an Airy[15] pattern. A careful comparison of Fig. 3(c) with a theoretical Airy distribution reveals the error between the two patterns to be less than 1% at any point. This error arises mainly from the problem of adequately representing a circular aperture with a rectangular array of samples.

Defocus

The aberration of defocus has the functional form $\Phi(r, \theta) = a_{20}r^2$, where the coefficient a_{20} is the amount of aberration. Defocus is the simplest type of aberration in that the real wave front differs from the spherical reference wave front only in its radius of curvature. A calculation of the amplitude impulse response, for the case when $a_{20} = 0.5$ wave, yielded the results shown in Fig. 4. In this figure the top two plots show the modulus (on the left) and the phase of the amplitude impulse response when the exit pupil of the optical system has a uniform transmittance, i.e., when there is no apodization. For ready comparison, the amplitude impulse response (modulus and phase) for the same system with a Gaussian apodizer is shown in the bottom two plots of the same figure.

The modulus and the phase of the unapodized amplitude impulse response (top two plots) should be compared with the analogous plots of Fig. 3 where there are no aberrations in the system. The peak value of the modulus in the aberrated case decreased relative to the unaberrated case. The zero values in the modulus pattern for the unaberrated case

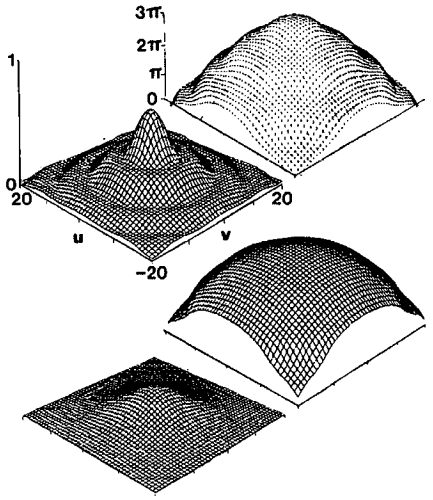

Fig. 4. The amplitude impulse response (modulus and phase) in the presence of 0.5-wave defocus and for the case of an unapodized and a Gaussian apodized aperture. The top two plots are for the unapodized case, and the bottom two are for the case of a Gaussian apodizer. The vertical scales for the modulus plots (left-hand column), and the phase plots (right-hand column) are indicated by the top two plots. The same scaling is used in Figs. 7, 10, and 13.

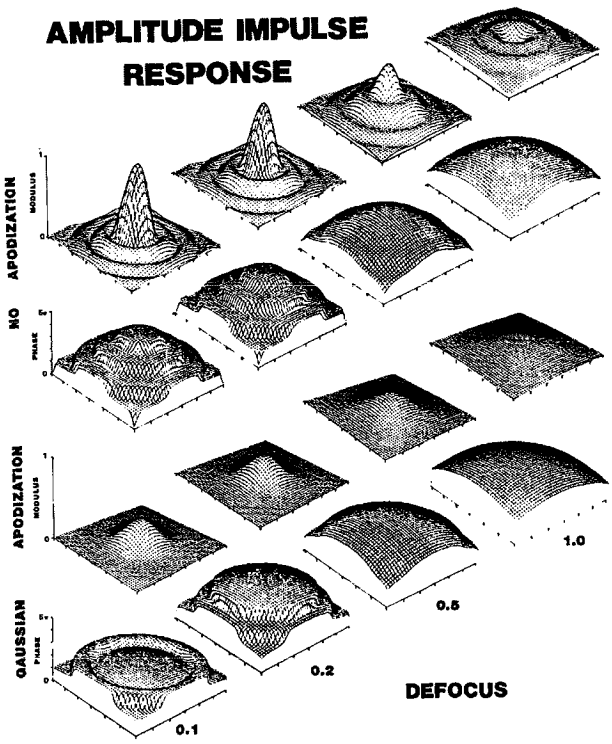

Fig. 5. The amplitude impulse response (modulus and phase) with varying amounts of defocus for the case of an unapodized and a Gaussian apodized exit pupil. The amount of aberration for each column is indicated at the bottom of that column.

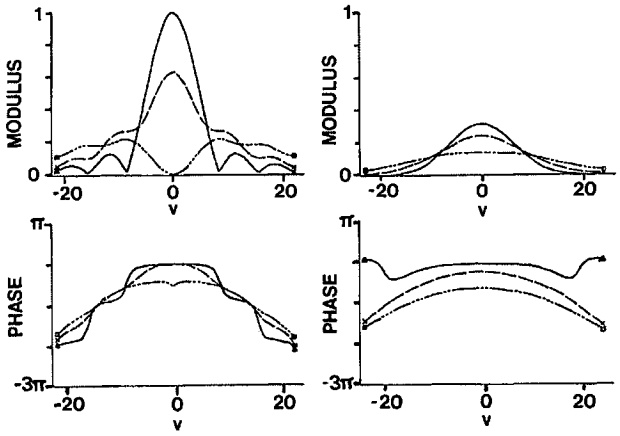

Fig. 6. Central slices through the plots of modulus and phase in the presence of varying amounts of defocus and for the unapodized (left-hand column) as well as the Gaussian apodized case: ——, 0.1 wave; — — —, 0.5 wave; — — — —, 1.0 wave.

evolved to relative minimums that do not go to zero. The phase of the aberrated amplitude impulse response (upper-right-hand plot of Fig. 4) no longer has the discontinuities evident in the unaberrated case.

When the apodizer described by Eq. (2) and plotted in Fig. 2 is applied to this aberrated system, the modulus of the amplitude impulse response (lower-left-hand plot of Fig. 4) is considerably smoothed, as is the phase. The phase varies by less than π rad over the region of the modulus plot where the modulus is greater than 10% of its peak value. So this amplitude impulse response does not change sign until the absolute value of the amplitude is quite small. Thus the impulse response is almost real and positive.

This has important implications for the imaging performance of optical systems. For instance, the ringing in the coherent image of an edge is caused by the negative regions of the impulse response. In this case the apodizer has smoothed the amplitude impulse response such that it has very little amplitude in the regions where there are negative values of amplitude. It can be expected, then, that the image of an edge through this system would be free from ringing.

The amplitude impulse response, both unapodized and apodized, for other values of defocus is shown in Fig. 5. Here the amount of aberration is different for each column of plots, varying from 0.1 wave on the left to 1.0 wave on the right. From these plots the evolution of the modulus and the phase can be seen as more defocus is added to the system.

The modulus and the phase along slices through the center of some of these impulse responses are shown in Fig. 6. The relationship of phase to modulus is clearly seen in this figure.

Apodization, in each case of the last three figures, smoothes both the modulus and the phase. In each case, the amplitude impulse response becomes almost real and positive when the apodizer is applied. There are, however, limits to this process. As the amount of aberration increases, the apodizer becomes less effective in making the amplitude impulse response almost real and positive. For the case of one wave of defocus, it appears that the phase has changed by more than $\pi/2$ rad over the region where the modulus is still relatively large.

Spherical Aberration

Spherical aberration has the functional form $\Phi(r, \theta) = a_{40}r^4$. Spherical aberration, like defocus, is a radially symmetric aberration. Owing to its fourth-power dependence on the radial distance parameter r, spherical aberration describes a

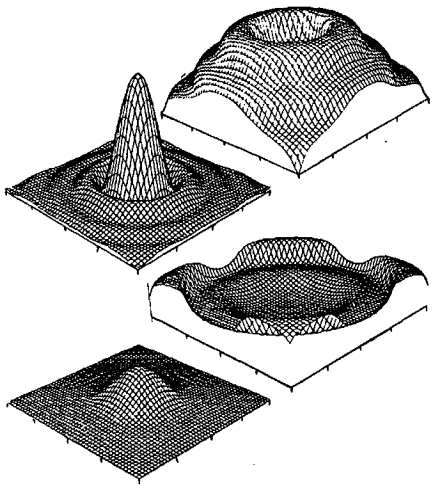

Fig. 7. The amplitude impulse response (modulus and phase) in the presence of 0.5-wave spherical aberration and for the case of an unapodized and a Gaussian apodized aperture. The top two plots are for the unapodized case, and the bottom two are for the case of a Gaussian apodizer. See Fig. 4 for the scaling.

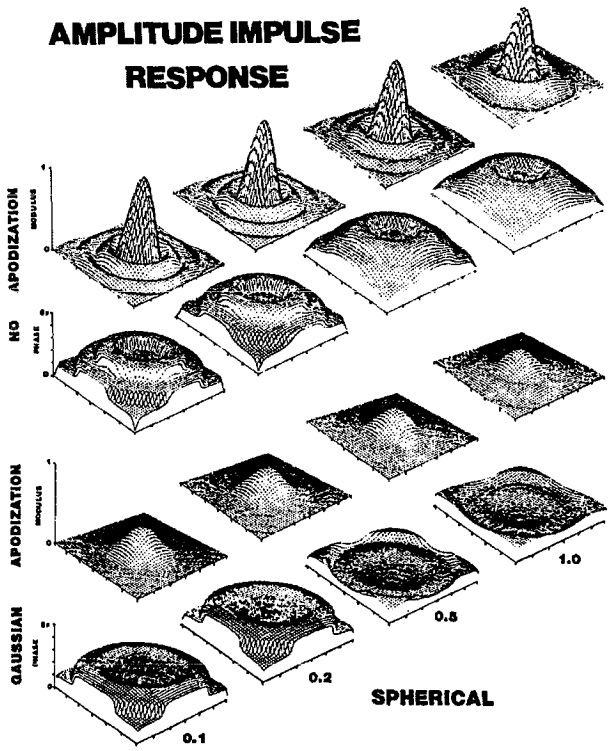

Fig. 8. The amplitude impulse response (modulus and phase) with varying amounts of spherical aberration for the case of an unapodized and a Gaussian apodized exit pupil. The amount of aberration for each column is indicated at the bottom of that column.

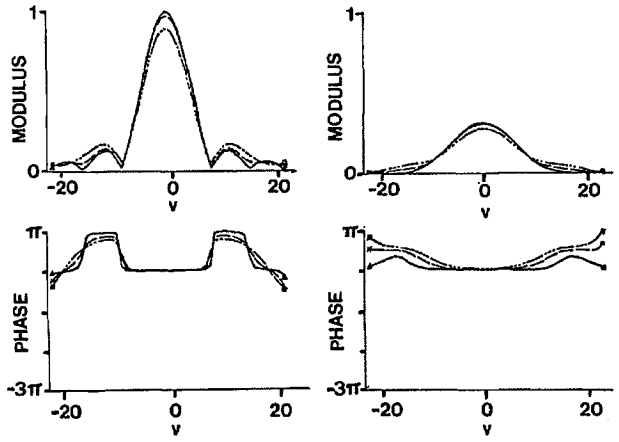

Fig. 9. Central slices through the plots of modulus and phase in the presence of varying amounts of spherical aberration and for the unapodized (left-hand column) as well as the Gaussian apodized case: ——, 0.1 wave; — — —, 0.5 wave; — — — —, 1.0 wave.

wave front having the largest deviation from the spherical reference wave front of any of the aberrations considered. A calculation of the impulse response (modulus and phase) when $a_{40} = 0.5$ wave is shown in Fig. 7. The top two plots (the unapodized case) should be compared with the unaberrated impulse response of Fig. 3. The presence of spherical aberration causes a decrease in the value of the central peak (Strehl ratio) and an increase in the energy in the sidelobes, particularly the first sidelobe. The position of the ring of minimum values between the central lobe and the first sidelobe changes little for this value of aberration.

The impulse response when the apodizer is employed is shown in the bottom two plots of Fig. 7. As in the case of defocus, the use of the apodizer has resulted in a much smoother impulse response. An examination of the phase distribution shows that the phase is nearly uniform over the region of the impulse response having significant amounts of energy. This impulse response can also be described as being almost real and positive.

The evolution of the unapodized and apodized amplitude impulse responses as more spherical aberration is added to the system is shown in Fig. 8. Central slices through some of these plots are shown in Fig. 9. The same general phenomena seen in the case of defocus are seen here as well. The use of the apodizer results in an impulse response that is free from sidelobes in the modulus pattern and that has a relatively flat phase over the region where there is a significant amount of energy.

Again there are limits to this process. When the amount of spherical aberration is about one wave, the impulse response has significant amounts of energy in regions where the phase has changed by about $\pi/2$. So the apodizer is not totally effective, although the apodized impulse response is still much smoother than the unapodized one.

Coma

The aberration of coma can be described by $\Phi(r, \theta) = a_{31} r^3 \cos\theta$. Coma is the first aberration considered for which the wave front in the exit pupil depends on the polar angle as well as on the radial distance r. This aberration therefore produces the unsymmetrical amplitude impulse response seen in Fig. 10 for the case $a_{31} = -0.5$ wave. The use of the apodizer in this case appears to be less effective than in the previous cases, because the first sidelobe is still evident in the modulus of the apodized impulse response (lower-left-

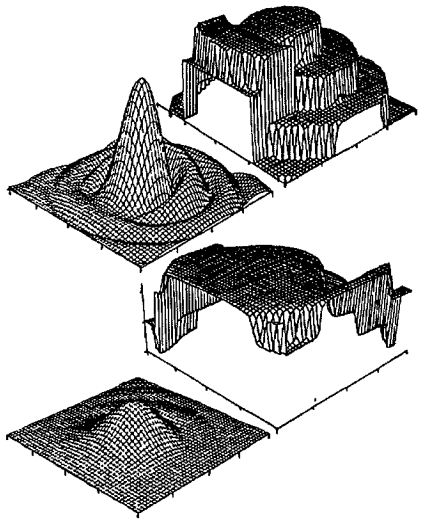

Fig. 10. The amplitude impulse response (modulus and phase) in the presence of −0.5-wave coma and for the case of an unapodized and a Gaussian apodized aperture. The top two plots are for the unapodized case, and the bottom two are for the case of a Gaussian apodizer. See Fig. 4 for scaling.

DOCKET ALARM

Explore Litigation Insights

Docket Alarm provides insights to develop a more informed litigation strategy and the peace of mind of knowing you're on top of things.

Real-Time Litigation Alerts

Keep your litigation team up-to-date with **real-time alerts** and advanced team management tools built for the enterprise, all while greatly reducing PACER spend.

Our comprehensive service means we can handle Federal, State, and Administrative courts across the country.

Advanced Docket Research

With over 230 million records, Docket Alarm's cloud-native docket research platform finds what other services can't. Coverage includes Federal, State, plus PTAB, TTAB, ITC and NLRB decisions, all in one place.

Identify arguments that have been successful in the past with full text, pinpoint searching. Link to case law cited within any court document via Fastcase.

Analytics At Your Fingertips

Learn what happened the last time a particular judge, opposing counsel or company faced cases similar to yours.

Advanced out-of-the-box PTAB and TTAB analytics are always at your fingertips.

API

Docket Alarm offers a powerful API (application programming interface) to developers that want to integrate case filings into their apps.

LAW FIRMS
Build custom dashboards for your attorneys and clients with live data direct from the court.

Automate many repetitive legal tasks like conflict checks, document management, and marketing.

FINANCIAL INSTITUTIONS
Litigation and bankruptcy checks for companies and debtors.

E-DISCOVERY AND LEGAL VENDORS
Sync your system to PACER to automate legal marketing.